

§16. Study of an Impurity Transport in Divertor Plasma with Use of TPD-II

Sugimoto, T., Matsubara, A., Sato, K., Sudo, S.

In divertor plasmas (a region from a scrape-off or ergodic layer to a divertor plate), characterizing the impurity flows is important for understanding energy balance under the convection-dominated condition. It is pointed out that the transport of impurity ions in the divertor plasma is strongly affected by collisions with the working gas ions (friction) and temperature gradient forces. However, there are many subjects that are not yet solved. In LHD plasma, a significant reduction of metallic impurity radiation was observed with changing the divertor plate from stainless steel into carbon. This suggests that the backstreaming into the plasma core was the main sources of the metallic impurity in the LHD divertor configuration. The question is whether impurity backstreaming actually occurs in the divertor plasma.

Simulation experiments for impurity transport are conducted in the TPD-II (Test Plasma by Direct current discharge) facility at NIFS. The schematic diagram of the TPD-II is shown in Fig. 1. TPD-II is a steady-state high-density plasma ($N_e \sim 10^{14} \text{ cm}^{-3}$ and $T_e \sim 10 \text{ eV}$) source. The plasma is produced with discharge current of more than 100A, and blows out from the anode hole ($\phi=8\text{mm}$) with flow velocity of $10^5 \sim 10^6 \text{ cm/s}$. The plasma is sustained with magnetic field of 3kG and terminates on a target.

We investigated the spatial distributions of carbon emissions along the He plasma column of 2m in length. The observed result is shown in Fig. 2. In front of the carbon target, strong spectrum line of CI (2479Å) was observed. And this CI spectral intensity decreases immediately toward the upstream side. Associated with the disappearance of CI spectra, CII (2837Å) and CIII (2297Å) spectra turn up successively at the upstream side.

As the TPD-II plasma is the steady plasma, the observed spatial distributions of carbon emission are attributed not only to the successive ionization of carbon flow from the carbon target source but also recombination processes of carbon ions which flow into the target. An example of a calculation result using continuity equation (1) only in consideration of is shown in Fig. 3, where atomic processes of ionization and recombination are only considered. We are going to analyze further about the observed spatial distributions with a 1-dimensional transport model that includes a friction and temperature gradient force.

$$\frac{\partial}{\partial Z} (N_{C^{+n}} v_{C^{+n}}) = N_e N_{C^{+n-1}} R_{C^{+n-1} \rightarrow C^{+n}} - N_e N_{C^{+n}} R_{C^{+n} \rightarrow C^{+n+1}} - N_e N_{C^{+n}} \alpha_{C^{+n} \rightarrow C^{+n-1}} + N_e N_{C^{+n+1}} \alpha_{C^{+n+1} \rightarrow C^{+n}} \quad (1)$$

R: ionization rate coefficient
 α : recombination rate coefficient

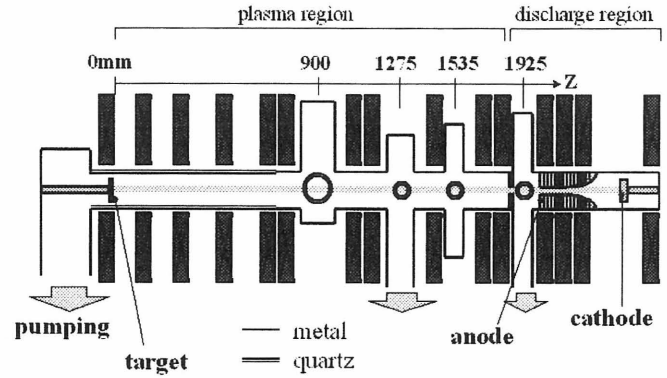


Fig. 1. Schematic diagram of the TPD-II.

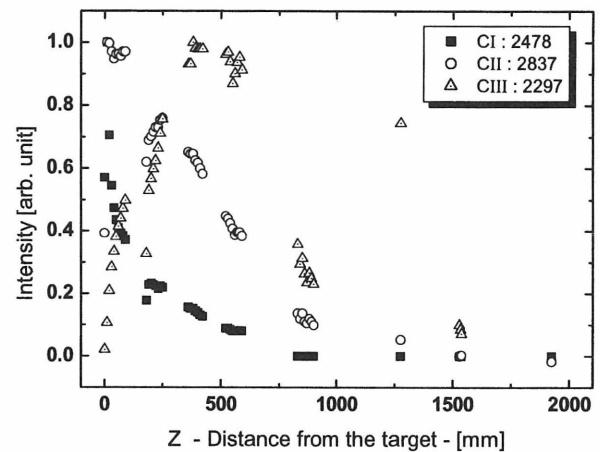


Fig. 2. Spatial distributions of carbon emissions along the He plasma column.

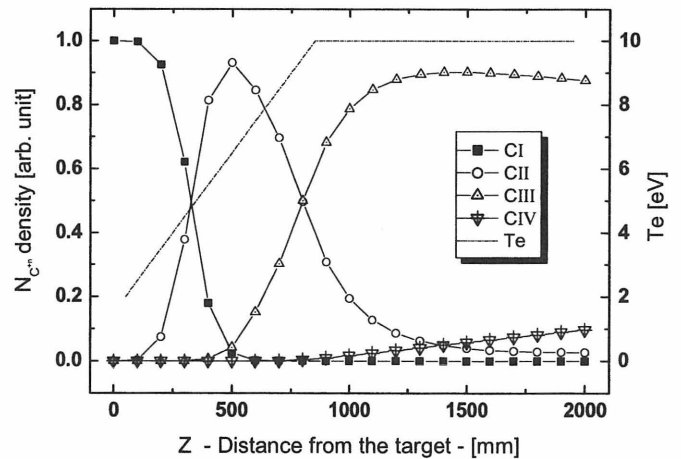


Fig. 3. Calculation results using eq. (1).
 $N_e (=5 \times 10^{12} \text{ cm}^{-3})$ and $v_{C^{+n}} (=10^5 \text{ cm/s})$ are constant.